JAAS

Accepted Manuscript

This is an *Accepted Manuscript*, which has been through the Royal Society of Chemistry peer review process and has been accepted for publication.

Accepted Manuscripts are published online shortly after acceptance, before technical editing, formatting and proof reading. Using this free service, authors can make their results available to the community, in citable form, before we publish the edited article. We will replace this *Accepted Manuscript* with the edited and formatted *Advance Article* as soon as it is available.

You can find more information about *Accepted Manuscripts* in the Information for Authors.

ROYAL SOCIETY OF CHEMISTRY

www.rsc.org/jaas

The determination of mercury in mosses by a novel cold vapor generation atmospheric pressure glow microdischarge optical emission spectrometry after the multivariate optimization

Krzysztof Greda,[a,*] Konrad Kurcbach,[a] Katarzyna Ochromowicz,[a] Tomasz Lesniewicz,[b] Piotr Jamroz,[a] Pawel Pohl[a]

[a] Wroclaw University of Technology, Faculty of Chemistry, Division of Analytical Chemistry and Chemical Metallurgy, Wybrzeze Stanislawa Wyspianskiego 27, 50-370 Wroclaw, Poland

[b] OpEx (Six Sigma) Master Black Belt Independent Consultant, Klodzka 1F/1, 55-040 Bielany Wroclawskie, Poland (e-mail: tomasz.lesniewicz@gmail.com)

*Corresponding author. Tel.: +48-71-320-3807, fax: +48-71-320-2494.
E-mail address: krzysztof.greda@pwr.edu.pl (K. Greda).

Abstract

A novel atmospheric pressure glow microdischarge system coupled with chemical vapor generation was applied to the optical emission spectrometry determination of Hg in samples of mosses (*Pleurozium schreberi*) from parks and surrounding forests of Wroclaw (Poland). The design of experiment (DOE) was used to optimize operating parameters of the microdischarge combined with a reaction/separation unit used for the chemical vapor generation. Seven experimental factors were examined, *i.e.*, concentrations of $NaBH_4$ and HCl, the discharge current and flow rates of reagents, the jet-supporting gas, the shielding gas and the liquid cathode solution, on the intensity of the Hg I 253.7 nm emission line and the standard deviation of background in its vicinity. Optimized operating conditions allowed to obtain the detection limit for Hg of 0.066 μg L^{-1} that was close to the predicted value with a fitted model. To separate Hg species from moss samples, a 2-step extraction procedure with a 5.0 mol L^{-1} HCl solution was carried out instead of the complete wet digestion with concentrated HNO_3. To validate the reliability of results, the spike-and-recovery experiment was performed. Obtained results were close to 100% proving the good accuracy of the methodology proposed. The average concentration of Hg in mosses in the urban area of Wroclaw was high (0.37 μg g^{-1}) but no specific source of contamination was found.

1. Introduction

The tracking of changes in the environment pollution caused by human activities is a matter of a great importance for contemporary analytical chemistry. Due to extremely high toxicity, Hg is the element of a particular interest. A lot of effort is currently being made to quantify Hg in food and relevant environmental samples such as waters,[1-3] lichens,[4-7] mosses[5-9] and mushrooms[10,11]. Apparently from the literature, except for commercially available inductively coupled (ICP) or microwave induced (MIP) plasma-based optical emission spectrometric (OES) instruments used to determine traces of Hg, there are concurrently some innovative plasma sources developed that have the same analytical performance as ICP or MIP but much smaller sizes and need much lower operation costs.[12-14] One of the most interesting devices is low-power capacitively coupled microplasma (μCCP) combined with cold vapor generation (CVG) that has been intensively explored for OES by Frentiu and co-workers.[15-20] The detection limit (DL) of Hg obtained with μCCP is of order of tens ng per L[15,16] and can be improved by using an additional pre-concentration system[17,18]. Other alternative low-power miniaturized plasma- or discharge-based radiation sources, including pulsed direct current microplasma (Pdc),[21] dielectric barrier discharge (DBD),[22-26] microwave microstrip plasma (MSP),[27,28] electrolyte cathode glow discharge (ELCAD)[29-31] or atmospheric pressure glow microdischarge (APGD)[32], are also developed and used for the determination of traces of Hg that is commonly pre-concentrated prior to spectrochemical measurements by using chemical vapor generation (CVG) systems,[15-19,21-23,25-28,32] sono-induced CVG,[20] a Au-on-W coiled filament,[24] or a solid phase extraction (SPE) tube[31].

In our recent paper,[32] a miniaturized atmospheric pressure glow discharge (μAPGD) generated between a miniature He flow jet nozzle anode and a small-sized flowing liquid cathode (FLC) was successfully combined with CVG for the OES quantification of traces of Hg. The DL of Hg evaluated with the system was 0.14 μg L^{-1} and it was quite promising bearing in mind that no trapping system for Hg vapors was used, while the integration of signals was short, *i.e.*, 0.1 s. Unfortunately, using optimal working parameters selected with a one-factor-at-a-time (OFAT) approach, the consumption of discharge supporting and shielding He gases was rather high and exceeded 2.5 L min^{-1} in total. Hence, in this paper, a novel, modified discharge chamber of lower dimensions was proposed to overcome the disadvantage of a high gas consumption. In addition, operating parameters of the CVG-μAPGD system were selected by a design of experiment (DOE) approach, simultaneously testing all important factors of the system. In the overwhelming majority of papers related to new

miniaturized plasma- or discharge-based radiation sources, the OFAT method was favored and applied to test the effect of different factors and select their optimal working conditions.[15-32] Although it is the most popular and generally accepted experimental approach, it requires more individual experiments to be run to achieve the desired precision of important effects of factors, cannot estimate interactions between factors and often misses their optimal settings.[33] Because the discharge phase is loaded with products (Hg vapor) and by-products (excess of H_2, H_2O vapor) of the CVG reaction, which takes place in a reaction/separation unit, a large number of experimental factors affect the performance of CVG-μAPGD-OES and numerous interactions could be expected.

Therefore, the present work was intended to find optimal conditions of the CVG-μAPGD system, reached at a global optimum and providing a maximum intensity of the analytical line of Hg as well as a minimal background level and its fluctuation in the vicinity of this line. To ensure this, it was necessary to simultaneously vary all factors by using the DOE method. Under optimized conditions, the CVG-μAPGD-OES system for the determination of Hg was validated and used to analyze samples of mosses. Instead of the complete wet digestion, samples were extracted using a 5.0 mol L^{-1} HCl solution. As a result, a fast and low-cost analytical methodology for measurements of total Hg in mosses was developed and applied to estimate the level of the Hg pollution in Wroclaw, a capital city of the Lower Silesian region in Poland.

2. Experimental

2.1. Instrumentation

A scheme of the μAPGD system generated between a He microjet nozzle anode and a small-sized capillary FLC is presented in Fig. 1. As compared to a recently described APGD system,[28] the present one was changed by reducing dimensions of a quartz discharge chamber (OD/ID 12/10 mm) and a quartz delivery capillary (OD/ID 4.0/2.0 mm). In a consequence, the volume of the chamber was merely 5 mL that is 50-fold lower than the volume of the previous one. This modification was to reduce the consumption of the shielding He gas. The solution of the FLC (0.1 mol L^{-1} HCl) was delivered through the quartz capillary using a 2-channel LabCraft, model Hydris 05, peristaltic pump (France). Unlike in the previous system,[32] an additional graphite tube, typically mounted onto the top of the quartz capillary and connected to a Pt wire, was not applied. This allowed to reduce the risk of the diffusion of

H_2 into the discharge. The overflowing solution dripped to the bottom of the quartz chamber (5 mL) and was drained out with the same peristaltic pump. The jet-supporting gas (He) was introduced through a stainless steel nozzle (length 35 mm, OD/ID 1.20/0.75 mm) using a Tylan General (CA, USA) FC-2900 flow controller and a RO-28 digital flow meter. The nozzle and the quartz capillary were vertically oriented with a gap between them of 5.0 mm. The electric supply to a FLC solution was also completely changed. One Pt wire was attached to the steel nozzle, another one was placed in the waste solution reservoir at the bottom of the discharge chamber. Both wires were used to provide the electric contact to electrodes. A stable discharge was maintained when a miniature He flow was passed through the nozzle while a potential within 900-1400 V was supplied from a HV dc power supply (Dora, Poland) to electrodes. A resultant discharge current of 15-45 mA was stabilized by a 5 kΩ ballast resistor. To prevent μAPGD zones from penetrating by the ambient air and deteriorating excitation conditions, a flow of the He shielding gas was applied and controlled by a rotameter. The shielding gas flowed out the discharge chamber through an elliptical hole (IDs 8 and 5 mm) that was also used to monitor the discharge.

A continuous flow CVG system has already been described in details in our recent paper.[32] Cold vapor of Hg along with H_2 and H_2O vapor were swept from the reaction/separation unit by the carrier/jet-supporting gas (He) and introduced into the near-anode region of μAPGD through the stainless steel nozzle. Reagents for the CVG reaction, *i.e.*, $NaBH_4$ and acidified sample/standard solutions, were delivered at the same flow rate, using the second peristaltic pump.

The emitted radiation from the near-anode region of μAPGD loaded with vapor of Hg was detected using a Triax 320 spectrometer (Horiba-Jobin Yvon, France). The spectrometer had a holographic grating (1200 grooves/mm). Emission spectra of the discharge were acquired using a 0.01 nm step and an integration time of 0.5 s. Profiles of the Hg I 253.7 nm emission line were recorded in ~1.0-1.5 nm spectral windows. Further details on the optical detection arrangement are described in ref. 32.

In addition, an Agilent bench-top optical emission spectrometer, model 720, with an axially-viewed Ar ICP and a 5-channel peristaltic pump was used to measure the concentration of Hg in solutions of digested samples of a selected moss. The ICP-OES instrument was equipped with a high-resolution echelle-type polychromator and a VistaChip II CCD detector cooled down to -35 °C on a triple-stage Peltier device. The plasma was sustained in a standard, one-piece, extended quartz torch with an injector tube of 2.4 mm ID. A single-pass glass cyclonic spray chamber and an OneNeb pneumatic concentric nebulizer

made of a high-tech PFA and PEEK polymers were used to introduce solutions of samples and standards by the pneumatic nebulization. Operating conditions recommended by the manufacturer for aqueous solutions containing high levels of dissolved-solids were applied, *i.e.*, the RF power of 1200 W, the plasma gas flow rate of 15.0 L min^{-1}, the auxiliary gas flow rate or 1.5 L min^{-1}, the nebulizer gas flow rate of 0.75 L min^{-1}, the sample uptake rate of 0.75 mL min^{-1}, the stabilization delay of 15 s, the sample uptake delay of 30 s, the rinse time of 10 s, the replicate read time of 1 s, the number of replicates of 3. The Hg I 184.9 nm emission lines was selected for measurements. A fitted background mode with 7 points per a line profile was applied for the background correction. Background corrected intensities of analytical lines were used for the calibration. The detection limit of 0.88 μg L^{-1} of Hg was evaluated for this analytical line.

2. 2. Reagents and solutions

Doubly distilled water was used throughout the work. He (99.999% grade) was delivered by Air Products (Poland). A stock standard solution of Hg (1000 mg L^{-1}), NaOH and $NaBH_4$ were supplied by Sigma-Aldrich. Standard solutions of 100 μg L^{-1} of Hg were prepared by appropriate dilutions of the stock standard solution. To stabilize solutions of the reducing agent, solid $NaBH_4$ was dissolved in a 0.1% *m/V* NaOH solution. The solution of $NaBH_4$ was freshly prepared and filtered through a cellulose filter paper. A concentrated HCl solution (high purity, dedicated to determinations of Hg) was obtained from Sigma-Aldrich and used to acidify all solutions of standards and samples. In addition, concentrated HNO_3 (J. T. Baker) and 30% *m/m* H_2O_2 (Sigma-Aldrich) solutions were used for the open-vessel wet oxidative digestion of samples of mosses. All reagents were of analytical grade or better.

2.3. Procedures

2.3.1. Design of experiments and Kriging estimation

To optimize operating parameters of the CVG-μAPGD system, a Box-Behnken design with 64 runs (randomized and including 8 center points) was used. All measurements, related to the intensity of the Hg I 253.7 nm emission line and the standard deviation of background (SDB) in its vicinity, were repeated 3 times and averaged. Seven experimental factors were defined, *i.e.*, the concentration of $NaBH_4$ (0.005-0.05% *m/V*), the concentration of HCl used for the acidification of solutions of samples and standards (3.0-6.0 mol L^{-1}), the flow rate of reagents' (reducing agent and sample/standard) solutions (0.6-6.0 mL min^{-1}), the discharge current (15-45 mA), the flow rate of the jet-supporting gas (0.06-0.30 L min^{-1}), the flow rate of the

shielding gas (0-2.0 L min^{-1}) and the flow rate of the FLC solution (0.9-2.1 mL min^{-1}), necessary for sustaining the discharge. To describe main effects, interactions and a curvature of these factors on the response of the system, *i.e.*, the intensity of the Hg emission line and the SDB, a quadratic model was chosen. Responses of the system were analyzed using Minitab 17 for Windows 7 (32-bit). The same software was used to create and verify models describing the response of the CVG-µAPGD system.

A two-dimensional Kriging estimation was used to determine the most likely spatial distribution of the concentration of Hg over the urban area of Wroclaw, Poland. An ordinary Kriging regression model was used for predicting intermediate values for the selected territory in reference to the data assessed during the spectrochemical analysis (using CVG-µAPGD-OES) of samples of mosses collected in different 31 points accros the interpolated area. A Surfer 10 modeling package for Windows 7 (32-bit) was used in this case for the purpose of the modeling of the concentration of Hg in the Wroclaw territory. Such an approach was previously used to predict the concentration of Hg over different territories in reference to results of the analysis of sediments,[34] soil,[35]and biota.[36,37]

2.3.2. Samples and their preparation

Thirty one samples of mosses (*Pleurozium schreberi*) were collected in parks and surrounding forests of Wroclaw, the capital city of the Lower Silesia region (Poland) in a period from July to October 2014. There are several potential sources of the pollution with Hg in the studied area, namely a coal thermal power plant, several food factories, pharmaceutical and chemical industries and numerous highways and motorways. In each location, sampling was done at 5-6 individual places within a radius of 10 m. All sub-samples from one location were mixed in a polyethylene container to form a gross sample. Gross samples were cleaned from any adhering particles and the soil but they were not rinsed with water. Dried samples were milled to a fine powder in an agate planetary ball mill, model Pulverisette 7 (Fritsch, Germany) and sieved through a 200 µm sieve.

To extract Hg from mosses, portions of sieved samples (0.4 g) were weighted into 30-mL PE conical centrifuge tubes and 10.0 mL of a 5 mol L^{-1} HCl solution was added. Tubes were tightly closed and shaken for 1 h (at 50 ^{o}C) in a water bath shaker, model 357 (Elpan, Poland). Next, tubes with leachates were placed in a centrifuge, model 350 (MPW Medical Instruments, Poland), and centrifuged for 8 min at 7000 rpm. Resulting supernatants were transferred to 30-mL PE capped containers. Residual samples of mosses were treated with another 10.0 mL portions of a 5.0 mol L^{-1} HCl solution and the whole procedure described

above (including the extraction and the centrifugation) was repeated. Resulting supernatants were mixed with extracts from the first step. Finally, they were filtrated through cellulose filter papers; filtrates (~20 mL of acidic extracts of mosses) were kept for the spectrochemical analysis by CVG-µAPGD-OES on the content of Hg.

To validate the accuracy of the extraction procedure, the obtained data on the Hg concentration in extracted samples were compared with results based on the analysis of digested samples of mosses. For this aim, 0.5 g samples of a selected moss were weighted into 50-mL glass beakers and treated with a concentrated HNO_3 solution (7.0 mL). Beakers were covered with watch glasses and left overnight for the pre-digestion at room temperature. Subsequently, resulted sample suspensions were refluxed under the cover on a hot plate at 80°C for about 3 h. Then, they were brought to boiling and heated for additional 3 h. During this step, another portion of a concentrated HNO_3 solution (3.0 mL) was added. After cooling, 1.0 mL of a 30% *m/m* H_2O_2 solution was added to resulting sample solutions and they were heated for next 30 min. Finally, samples were evaporated to the dryness (using an IR lamp), while residues were reconstituted with 25.0 mL of a 5.0 mol L^{-1} HCl solution (in case of the analysis by CVG-µAPGD-OES) or water (in case of the analysis by ICP-OES) and filtrated through cellulose filter papers. All sample solutions (extracts and digests) were prepared in triplicate, respective blank samples were run and considered in final results.

In addition, to verify accuracy of CVG-µAPGD-OES, a spike-and-recovery experiment was carried out. Samples of a selected moss were spiked with known amounts of Hg so as its concentration in extracted and digested sample solutions was increased by 10 µg L^{-1}. Concentrations of Hg in mentioned samples solutions (extracts and digests) were measured by CVG-µAPGD-OES using for the calibration simple standard solutions prepared in a 5.0 mol L^{-1} HCl solution.

3. Results and discussion

3.1. Multivariate optimization of CVG-µAPGD operating conditions

As described above, the appropriate design of experiments was created to analyze the impact of different experimental factors, *i.e.*, operating parameters of the CVG-µAPGD system, on the intensity of the Hg I 253,7 nm emission line and the SDB in its vicinity. According to the selected Box-Behnken design, 64 measurements were made and obtained results are shown in Fig. 2. This figure presents values of the response, *i.e.*, the intensity of the Hg analytical line

and the SDB in its vicinity, *versus* a randomized experimental run order. As can be seen, there is a lack of any trends or patterns in the data that indicates a fair stability of the CVG-μAPGD system and no effect of any drift errors.

3.1.1. Models of the intensity of the analytical line of Hg

In order to describe the effect of studied factors on the intensity of the analytical line of Hg, several different functions were considered. The best results were obtained when the following models were used, *i.e.*, with no transformation (NOT) of the response, with its decimal logarithm (LOG) or square root (SQRT) transformations. The significance of effects of studied factors on the intensity of the analytical line of Hg was estimated in the first place on the basis of Pareto plots of standardized effects (Fig. 3). As can be seen, in accordance with all 3 models, the most significant factors for the CVG-μAPGD system are flow rates of He shielding (F) and jet-supporting (E) gases in addition to the flow rate of reagents (C). The effect of the concentration of reagents, *i.e.*, $NaBH_4$ (A) and HCl (B) used for the acidification of sample solutions, and the discharge current (D) on the intensity of the analytical line of Hg was apparently smaller. The impact of the flow rate of the FLC solution (G) was either of a minor importance.

In the next step, all models were reduced to remove any insignificant terms (at α=0.05). Terms included in reduced NOT, LOG and SQRT models of the intensity of the analytical line of Hg are listed in Table 1 along with a comparison of R-statistics obtained for them. Small differences between R-squared and R-adjusted statistics indicate that all selected models were not over-fitted. Moreover, R-predicted values demonstrate that all 3 models can very well predict new observations. Concluding, it appears that each of fitted models quite correctly described the variability of the intensity of the analytical line of Hg, hence, all of them were considered in the further study.

3.1.2. Model of the standard deviation of background in the vicinity of the analytical line of Hg

In order to explore the impact of operating conditions on the SDB, untransformed data (NOT) were considered in the first approach. Other transformation models of the response, *i.e.*, LOG and SQRT, were also used. Unfortunately, results obtained for these models were unsatisfactory because R-statistics were quite low and a lot of outliers were observed on residual plots. To receive a better fitted model, the data related to the SDB were transformed to its reciprocal square root (RSQRT). The Pareto chart for the proposed RSQRT model is

shown in Fig. 3. As can be seen, the most significant factors that affect the SDB in the vicinity of the analytical line of Hg, and indirectly the DL of Hg, are the discharge current (D), the flow rate of the shielding gas (F) and the flow rate of the FLC solution (G). This could be explained by a special role of N_2 molecules from the air atmosphere in the production of NO radicals and the contribution of the latter molecules to an increase of the background intensity and its fluctuation.[28] Statistically significant factors were also the flow rate of the jet-supporting gas (E) and the concentration of reagents (A, B) used for the CVG reaction. The flow rate of reagents (C) was virtually negligible.

Based on the Pareto chart, the proposed model was reduced and all included terms in the reduced model are listed in Table 1. Although the effect of the concentration of HCl (terms B and BB) was statistically significant, it was excluded from the reduced model. This is because, it has been established that the concentration of HCl used in the CVG reaction did not have an influence on excitation conditions in APGD and hence, could not affect the SDB.[32] Interactions "$NaBH_4$ concentration–liquid cathode flow rate" (term AG) and "HCl concentration–jet-supporting gas flow rate" (term BE) seemed to be unreliable, thus, they were either excluded from the reduced model. The quality of the proposed RSQRT model for the SDB in the vicinity of the analytical line of Hg was verified by plotting residual graphs. As can be seen form Fig. 4, a normal probability plot of residuals was obtained, proving no unusual observations (outliers) or deviations from the normal distribution. Moreover, the plot of standardized residuals *versus* fitted values for the transformed model of the SDB (Fig. 4) had no unusual structure or obvious patterns. This confirmed the correctness of the proposed model for the SDB. Based on presented residual plots, it was concluded that there was no reason to reject the model.

3.2. Effects of main factors

Fig. 5 demonstrates the effect of main factors on the intensity of the analytical line of Hg (based on the NOT model) and the SDB in the vicinity of this line (based on the retransformed RSQRT model). It is important to notice that, for the simplicity of viewing, presented results do not take into account interactions between factors, hence, they have only an informative value.

Accordingly, the increase in the concentration of $NaBH_4$ resulted in a linear decrease in the intensity of the analytical line of Hg within the whole studied range of this factor, *i.e.*, 0.005-0.05% *m/V*. This finding was consistent with results reported in our recent work for a larger in size μAPGD,[32] where it was found that the $NaBH_4$ concentration of 0.005% *m/V* was

sufficient to reach an almost 100% efficiency of the CVG reaction for Hg. When the concentration of the reducing agent exceeded 0.005% *m/V*, only the amount of the concomitant H_2 by-product increased but the excitation capability of μAPGD studied here was obviously deteriorated. Simultaneously, the background intensity and its fluctuation increased in these conditions what was proved by the model proposed for the SDB. Considering all of this, it was expected that a low concentration of $NaBH_4$ would be desired. The optimal concentration of HCl was about 4.5 mol L^{-1} and this value was coincident with the concentration of HCl required for the extraction of Hg from samples of mosses. The increase in the flow rate of both reagents for the CVG reaction caused a strong enhancement of the signal of Hg, while the SDB in vicinity of the analytical line of Hg was virtually unchanged. For this reason, a high flow rate of reagents, *i.e.*, 5.5-6.0 mL min^{-1}, was preferred. The influence of the discharge current on the signal of Hg seemed to be counterintuitive but a similar observation was noted in our earlier study but for a greater in size μAPGD discharge chamber.[32] Accordingly, it could be expected that an increase in the discharge current would be responsible for an increase in the energy density and a boost of the signal of Hg. Surprisingly, it was found that the growth of the discharge current did not improve the intensity of the analytical line of Hg. It was even worse and an enormous increase in the SDB was observed as a result of an enhancement of the background intensity and a discharge destabilization. It is worth noting that the increase in the flow rate of the jet-supporting gas resulted in a reduction of the SDB despite an apparent increase in the background intensity. This observation clearly proved that the use of this gas stream stabilizes μAPGD. The greatest improvement of the intensity of the analytical line of Hg was established for a high flow rate of the shielding gas. Unfortunately, in these conditions μAPGD was concurrently destabilized what led to a high enhancement of the SDB, partially related to the observed growth of the background intensity.

3.3. Analytical performance and application

To find operating conditions of the CVG-μAPGD system that would provide the lowest DL of Hg, each of 3 models proposed for the intensity of the analytical line of Hg, *i.e.*, NOT, LOG, SQRT, was coupled with the transformed RSQRT model for the SDB. Compromised settings of factors were established by maximizing the intensity of the analytical line of Hg and minimizing the SDB. The concentration of HCl in this trial was kept constant at 5.0 mol L^{-1} (close to the optimal value) because the extraction of Hg from mosses sample was made with a solution of the same concentration. Other factors were continuously changed within the

whole examined ranges. As a result, 3 different optimal settings of factors (see Table 2) were obtained and validated in additional measurements (n=10 for each setup). A mean value of the DL of Hg achieved was 0.066±0.003 μg L^{-1}, while a respective mean value of the DL predicted by models used was 0.051±0.003 μg L^{-1}. The reason for this difference was possibly an inaccurate fit of models describing the intensity of the analytical line of Hg (measured intensities were by ~20% lower than expected values). Nevertheless, obtained results were the lowest out of all previously observed, hence, it was concluded that the applied DOE method made it possible to find optimal operating conditions of the CVG-μAPGD system for the determination of traces of Hg. There was no apparent difference between DLs of Hg achieved for each model but the LOG model was considered the most optimal and hence, it was used in further experiments because it required the lowest flow rate of the shielding gas.

For the calibration of the CVG-μAPGD-OES method, 10 standard solutions of Hg acidified with HCl (5.0 mol L^{-1}) were used and spanned the concentration range of 0.5-100 μg L^{-1}. The resulting calibration curve was linear (R^2>0.9995) within the whole mentioned concentration range. The overall precision (n=10), derived on the basis of measurements of all standard solutions, was 2.1% and did not exceed 3.8% in any case.

To evaluate the accuracy of results obtained for the proposed extraction procedure of Hg from mosses followed by CVG-μAPGD-OES measurements, concentrations achieved analyzing extracts and digests of one selected moss were compared. It was found that there was no statistically significant difference between mean concentrations of Hg determined in the same moss in sample solutions resulted from the extraction (0.40±0.02 μg g^{-1}) and wet the digestion (0.39±0.04 μg g^{-1}). It was also established that results determined in prepared sample solutions using CVG-μAPGD-OES (sample extracts) and ICP-OES (sample digests) did not differ from each other in a statistically significant manner according to the *t*-test at the 95.0% significance level (α=0.05). Finally, the recovery test was carried out. Determined recoveries of added Hg, when measuring solutions of digested and extracted samples of one selected moss, were within 102-109% and 91-107%, respectively. This confirmed the good accuracy of the proposed methodology, including both the alternative to the wet digestion the extraction procedure and the measurement CVG-μAPGD-OES method.

The proposed extraction procedure and the CVG-μAPGD-OES detection system were suitable for quantifying the total content of Hg in samples of mosses collected in different parts of the urban area of Wroclaw, the capital city of the Lower Silesia region, Poland. Based on results of the analysis of 31 samples of mosses, a distribution map of the concentration of

Hg in samples of mosses located in the whole selected urban area was modeled (Fig. 6). The content of Hg in analyzed mosses varied from 0.22 to 0.60 μg g^{-1} with an average value of 0.37 μg g^{-1} and the coefficient of variance (CV) of 28.5%. The precision of these measurements (n=3) was changed from 2.8 to 5.0% (as the relative standard deviation). This average value was much higher than the one obtained for low-urbanized areas.[7] Accordingly, Klos *et al.*[7] quantified the content of Hg in samples of mosses collected in several forested areas away from Wroclaw by about 100 km, and reported that the average concentration of this element accumulated in mosses was only 0.093 μg g^{-1}. The average concentration of Hg determined in mosses collected in Wroclaw and analyzed in the present work was comparable with that reported by Zawadzki *et al.*,[9] who analyzed samples collected in the vicinity of a chloral-alkali factory located in Brzeg Dolny (30 km away from Wroclaw). In our study, any apparent correlation between the level of Hg in mosses and the location of large industrial plants was not found. This could indicate that other sources of the pollution with Hg could contribute to the contamination of analyzed samples.

4. Conclusions

The use of the DOE statistical approach allowed to find optimal operating conditions of the novel CVG-μAPGD-OES detection system, where curvature and interactions between factors certainly occur. Under optimal conditions, the flow rate of the shielding He gas was only ~0.9 L min^{-1}, which is almost 3 times less than the setting used in our previous arrangement.[32]

Because of a reduced gas consumption, a low forward power (not exceeding 15 W) and the simplicity of the design and the operation of this system, it seems to be a low-cost and small in size Hg detector, alternative to large-scale spectrometric instruments, *e.g.*, ICP-OES or MIP-OES as well as CVG coupled with atomic fluorescence spectrometry (AFS) or atomic absorption spectrometry (AAS). The developed methodology offers the good precision and accuracy in addition to a high detectability of Hg.

The combination of the extraction procedure of mosses with a 5.0 mol L^{-1} HCl solution and the detection of Hg by CVG-μAPGD-OES brings a lot of benefits. The use of the simplified sample preparation leads to a lower risk of the contamination, which is of a great importance in case of the quantification of trace amounts of Hg in plant materials. On the other hand, the application of the miniaturized APGD excitation source for the detection of Hg results in inexpensive and simple analyses.

Acknowledgments

Research project co-funded by the Polish National Science Center (NCN) based on decision No. DEC-2013/09/N/ST4/00308. The work was also financed by a statutory activity subsidy from the Polish Ministry of Science and Higher Education for the Faculty of Chemistry of Wroclaw University of Technology.

References

1 E. K. Mladenova, I. G. Dakova, D. L. Tsalev and I. B. Karadjova, Cent. Eur. J. Chem., 2012, **10**, 1175–1182.

2 L. B. Escudero, R. A. Olsina and R. G. Wuilloud, Talanta, 2013, **116**, 133–140.

3 Q. Zhou, A. Xing and K. Zhao, J. Chromatogr. A, 2014, **1360**, 76–81.

4 O. Zverina, K. Laska, R. Cervenka, J. Kuta, P. Coufalik and J. Komarek, Environ. Monit. Assess., 2014, **186**, 9089–9100.

5 M. V. Balarama Krishna, M. Ranjit, D. Karunasagar and J. Arunachalam, Talanta, 2005, **67**, 70–80.

6 M. V Balarama Krishna, D. Karunasagar and J Arunachalam, Environ. Pollut., 2003, **124**, 357–360.

7 A. Klos, M. Rajfur, I. Sramek and M. Waclawek, Environ. Monit. Assess., 2012, **184**, 6765–6774.

8 G. Qiu, X. Feng, S. Wang and L. Shang, Appl. Geochem., 2015, **20**, 627–638.

9 K. Zawadzki, K. Sokolowska, A. Samecka-Cymerman, K. Kolon, A. Dubinska and A. J. Kempers, Ecotoxicol. Environ. Safe., 2014, **108**, 36–41.

10 I. Kula, M. H. Soylak, M. Ugurlu, M. Isiloglu, Y. Arslan, Bull. Environ. Contam. Toxicol., 2011, **87**, 276–281.

11 G. Jarzynska and J. Falandysz, J. Environ. Sci. Health, Part A, 2011, **46**, 569–573.

12 X. Yuan, J. Tang and Y. Duan, Appl. Spectrosc. Rev., 2011, **7**, 581–605.

13 J. Franzke, K. Kunze, M. Miclea and K. Niemax, J. Anal. At. Spectrom., 2013, **18**, 802–807.

14 J. Hu, W. Li, C. Zheng and X. Houa, Appl. Spectrosc. Rev., 2011, **6**, 368–387.

15 T. Frentiu, A. I. Mihaltan, M. Ponta, E. Darvasi, M. Frentiu and E. Cordos, J. Hazard.

Mater., 2011, **193**, 65–69.

16 T. Frentiu, A. I. Mihaltan, M. Senila, E. Darvasi, M. Ponta, M. Frentiu and B. P. Pintican, Microchem. J., 2013, **110**, 545–552.

17 T. Frentiu, A. I. Mihaltan, E. Darvasi, M. Ponta, C. Roman and M. Frentiu, J. Anal. At. Spectrom., 2012, **27**, 1753–1760.

18 T. Frentiu, S. Butaciu, E. Darvasi, M. Ponta, M. Senila, D. Petreus and M. Frentiu, Anal. Methods, 2015, **2**, 747–752.

19 T. Frentiu, S. Butaciu, M. Ponta, M. Senila, E. Darvasi, M. Frentiu and D. Petreus, Food Anal. Methods, 2015, **8**, 643–648.

20 T. Frentiu, S. Butaciu, E. Darvasi, M. Ponta, M. Senila, E. Levei and M. Frentiu, J. Anal. At. Spectrom., 2015, **30**, 1161–1168.

21 X. Yuan, G. Yang, Y. Ding, X. Li, X. Zhan, Z. Zhao and Y. Duan, Spectrochim. Acta Part B, 2014, **93**, 1–7.

22 Y. Yu, Z. Du, M. Chen and J. Wang, Angew. Chem. Int. Ed., 2008, **47**, 7909–7912.

23 Z. Zhu, G. C. Y. Chan, S. J. Ray, X. Zhang and G. M. Hieftje, Anal. Chem., 2008, **80**, 8622–8627.

24 M. Puanngam, S. Ohira, F. Unob, J. Wang and P. K. Dasgupta, Talanta, 2010, **81**, 1109–1115.

25 W. S. Abdul-Majeed, J. H. Lozano Parada, and W. B. Zimmerman, Anal. Bioanal. Chem., 2011, **401**, 2713–2722.

26 Y.-L. Yu, Y.-T. Zhuang and J.-H. Wang, Anal. Methods, 2015, **7**, 1660–1666.

27 P. Pohl, I. Jimenez Zapata, E. Voges, N. H. Bings and J. A. C. Broekaert, Microchim. Acta, 2008, **161**, 175–184.

28 V. Cerveny, M. Horvath and J. A. C. Broekaert, Microchem. J., 2013, **107**, 10–16.

29 R. Shekhar, D. Karunasagar, M. Ranjit and J. Arunachalam, Anal. Chem., 2009, **81**, 8157–8166.

30 R. Shekhar, Talanta, 2012, **93**, 32–36.

31 Q. Li, Z. Zhang and Z. Wang, Anal. Chim. Acta, 2014, **845**, 7–14.

32 K. Greda, P. Jamroz and P. Pohl, J. Anal. At. Spectrom., 2014, **29**, 893–902.

33 R. L. Mason, R. F. Gunst and J. L. Hess, Statistical Design and Analysis of Experiments, second ed., John Wiley & Sons, Inc., Hoboken, 2003.

34 Y. Ouyang, J. Higman, D. Campbell and J. Davis, J. Am. Water Resour. Assoc., 2013, **39**, 689–702

35 X. Yang and L. Wang, Environ. Geol., 2008, **53**, 1381–1388.

36 Z. Spiric, I. Vuckovic, T. Stafilov, V. Kusan and K. Baceva, Environ. Monit. Assess., 2014, **186**, 4357–4366.

37 R. Figueira, P. C. Tavares, L. Palma, P. Beja and C. Sergio, Environ. Pollut., 2009, **157**, 2689–2696.

Captions for figures

Fig. 1 The experimental set-up of μAPGD generated between a miniature He flow microjet and a small-sized flowing liquid cathode solution.

Fig. 2 Values of the intensity of the analytical line of Hg and the SDB in the vicinity of this line *versus* the run order.

Fig. 3 Standardized Pareto charts (α=0.05, $t_{critical}$=2.01) for the intensity of the analytical line of Hg (based on NOT, LOG and SQRT models) and the SDB in the vicinity of this line (based on the RSQRT model). A: $NaBH_4$ concentration. B: HCl concentration. C: Reagents flow rate. D: Discharge current. E: Jet-supporting gas flow rate. F: Shielding gas flow rate. G: Liquid cathode flow rate.

Fig. 4 The normal probability plot for the standardized residual distribution (based on RSQRT model for the SDB) (a) and the residual plot for the mentioned model presenting standardized residuals *versus* fitted values (b).

Fig. 5 The effect of main factors on the intensity of the analytical line of Hg and the SDB in its vicinity. A: $NaBH_4$ concentration. B: HCl concentration. C: Reagents flow rate. D: Discharge current. E: Jet-supporting gas flow rate. F: Shielding gas flow rate. G: Liquid cathode flow rate.

Fig. 6 The two-dimensional view of the distribution of the concentration of Hg in mosses in the urban area of Wroclaw, Poland.

Table 1. Statistically significant terms and the R-statistics for models describing the intensity of the analytical line of Hg and the standard deviation of the background (SDB) in its vicinity

		Intensity of the analytical line of Hg			SDB
		NOT	LOG	SQRT	RSQRT
Included terms	Linear	A, B, C, D, E, F	A, B, C, D, E, F	A, B, C, D, E, F	A, C, D, E, F,G
	Squared	CC, DD, EE	BB, CC, DD, EE, FF	BB, CC, DD, EE	DD, EE, GG
	Interactions	AD, CE, CF, DE	AD, BC, CE, CF, DE, EF	AD, CE, CF, DE, EF	AD, CF, FG
R-squared, %		84	92	89	87
R-adjusted, %		80	89	85	84
R-predicted, %		73	80	78	78

NOT No transformation of the response. LOG Logarithmic transformation of the response. SQRT Square root transformation of the response. RSQRT Reciprocal square root transformation of the response. A: $NaBH_4$ concentration. B: HCl concentration. C: Reagents flow rate. D: Discharge current. E: Jet-supporting gas flow rate. F: Shielding gas flow rate. G: Liquid cathode flow rate.

Table 2. Optimal operating conditions predicted on the basis of the SDB model coupled with different models for the intensity of the analytical line of Hg

	Model for the intensity of the analytical line of Hg		
	NOT	LOG	SQRT
$NaBH_4$ concentration, % $^{m/V}$	0.005	0.005	0.005
HCl concentration,[a] mol L^{-1}	5.0	5.0	5.0
Reagents flow rate, mL min^{-1}	5.73	5.45	6.00
Discharge current, mA	15	15	15
Jet-supporting gas flow rate, L min^{-1}	0.213	0.222	0.208
Shielding gas flow rate, L min^{-1}	1.82	0.89	1.54
Flowing liquid cathode flow rate, mL min^{-1}	1.34	0.90	1.11
Predicted DL, µg L^{-1}	0.051	0.053	0.048
Obtained DL, µg L^{-1}	0.066	0.066	0.071

[a] Kept constant at 5.0 mol L^{-1} (not optimized). DL Detection limit.

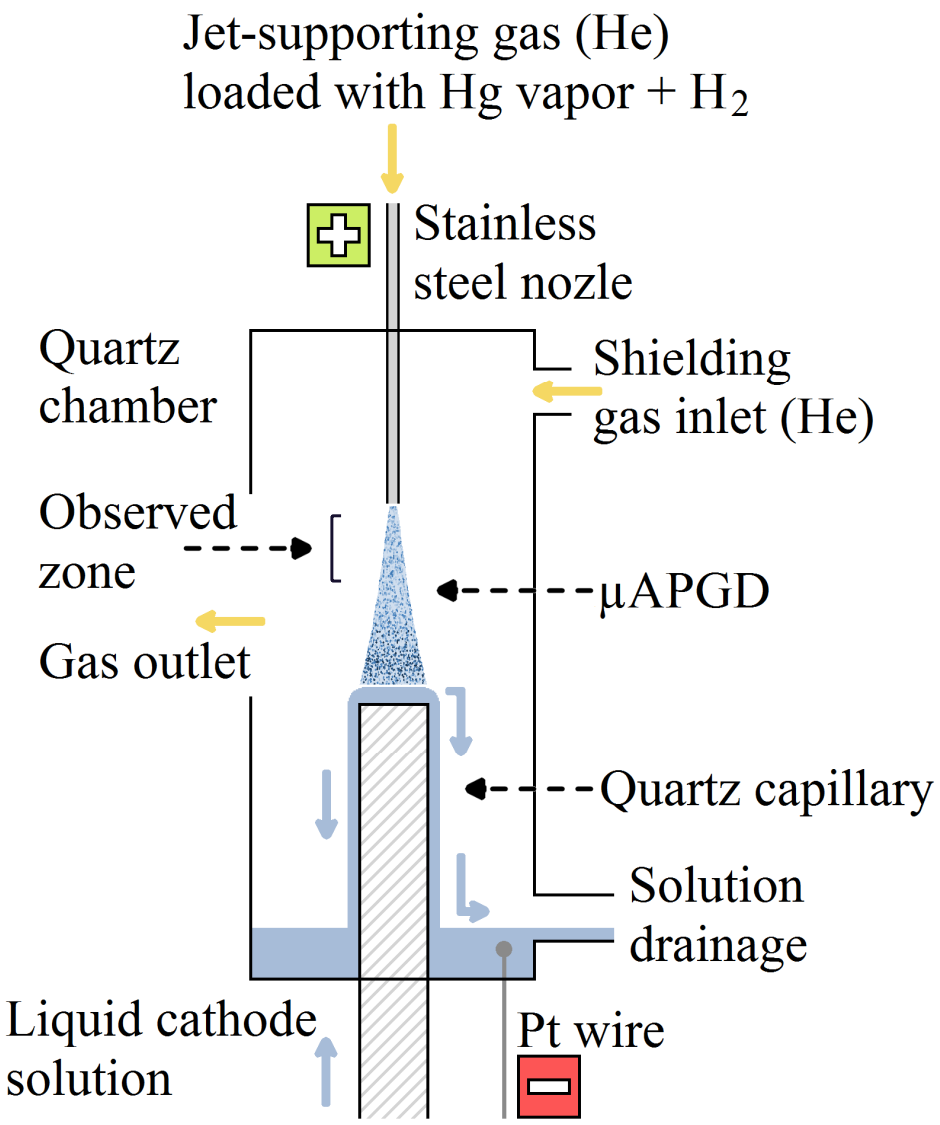

Fig. 1

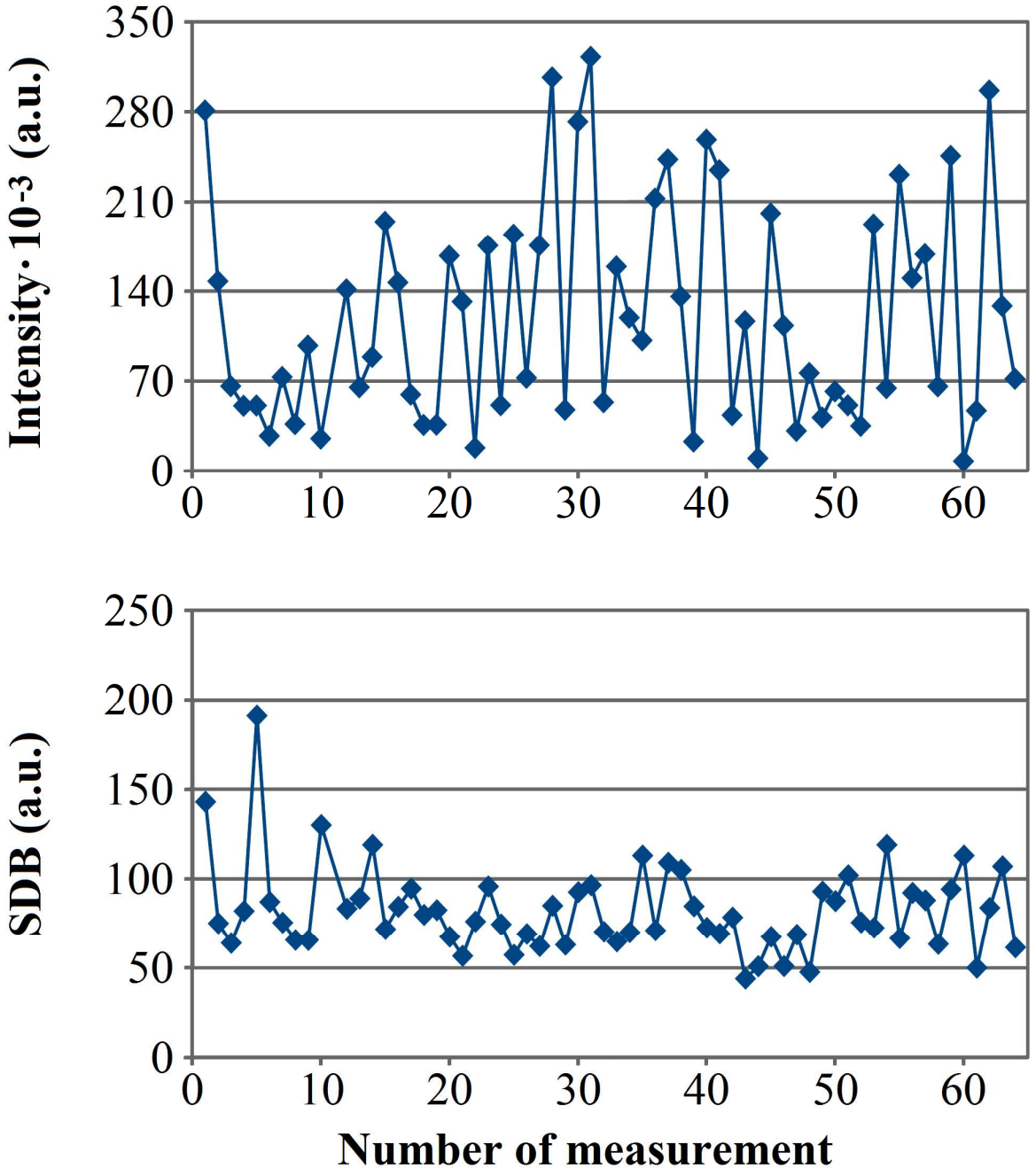

Fig. 2

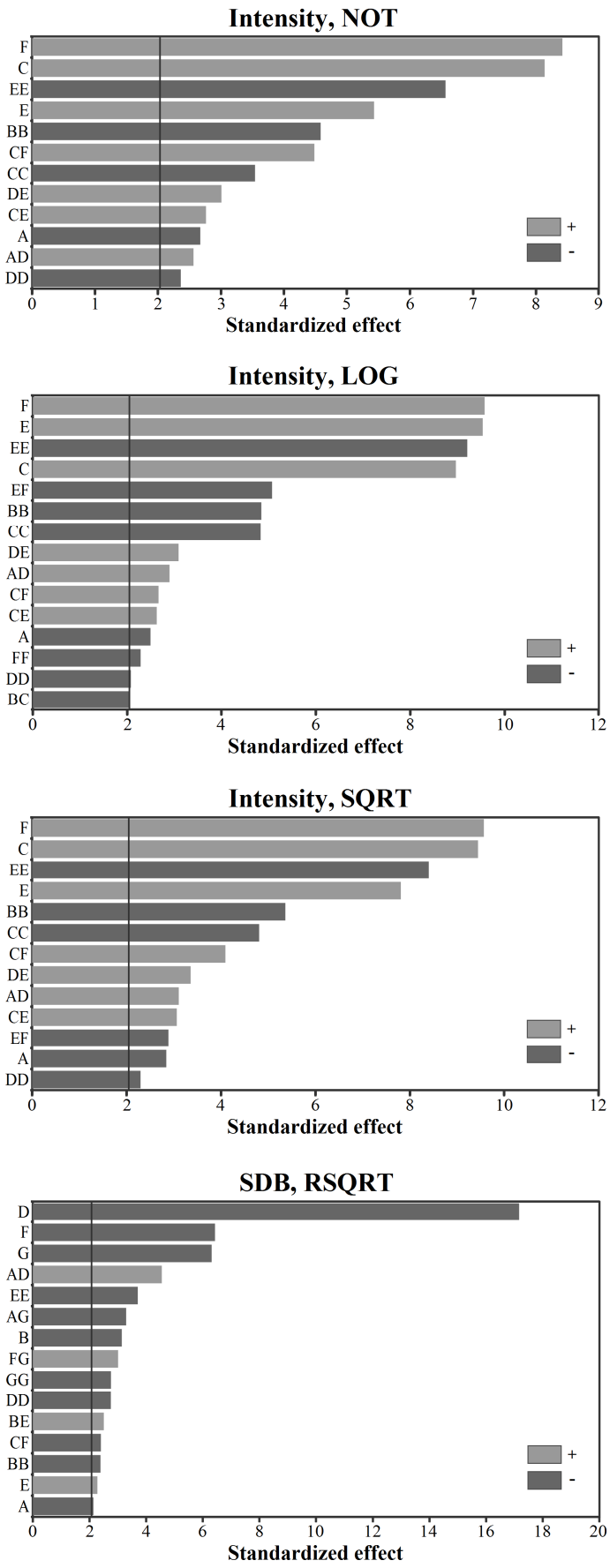

Fig. 3.

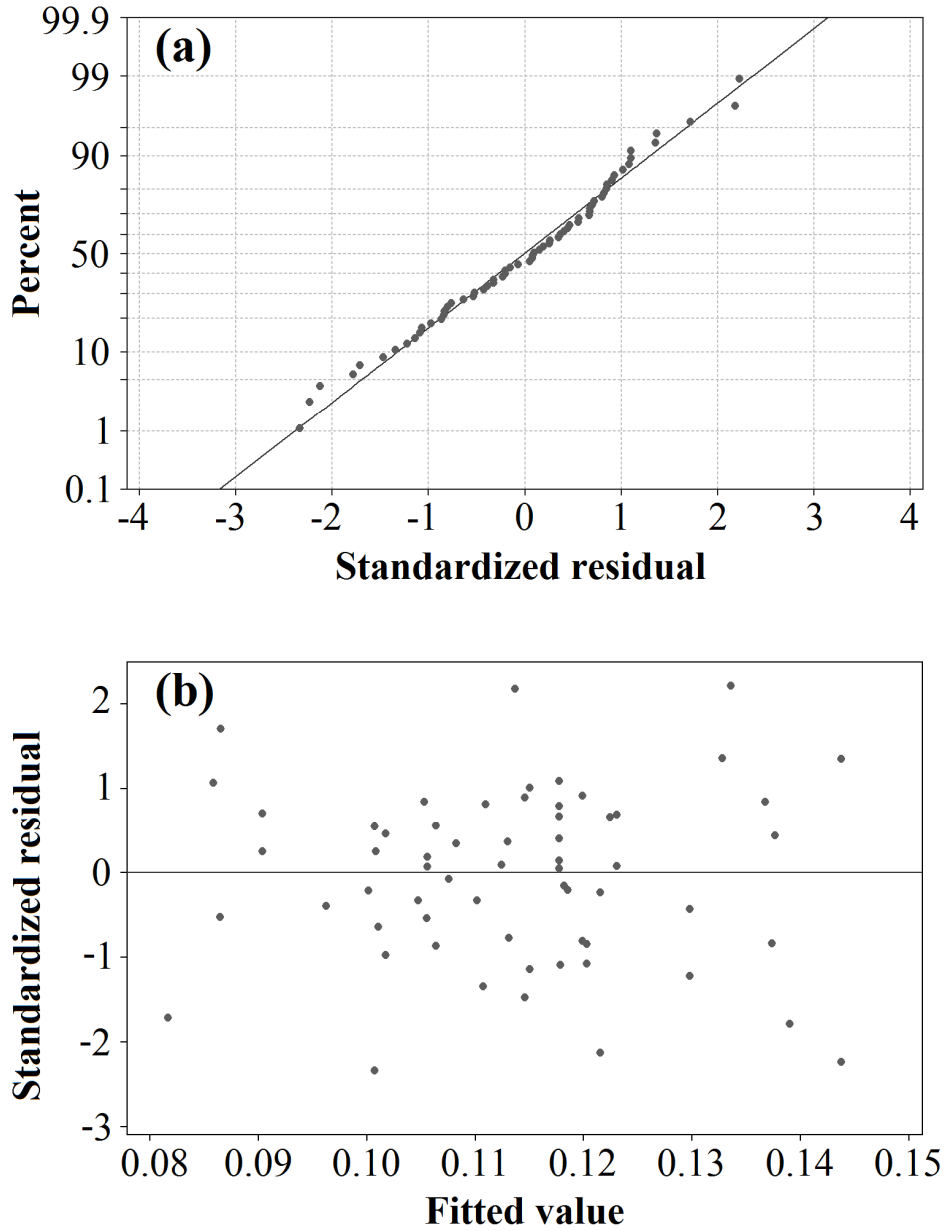

Fig. 4

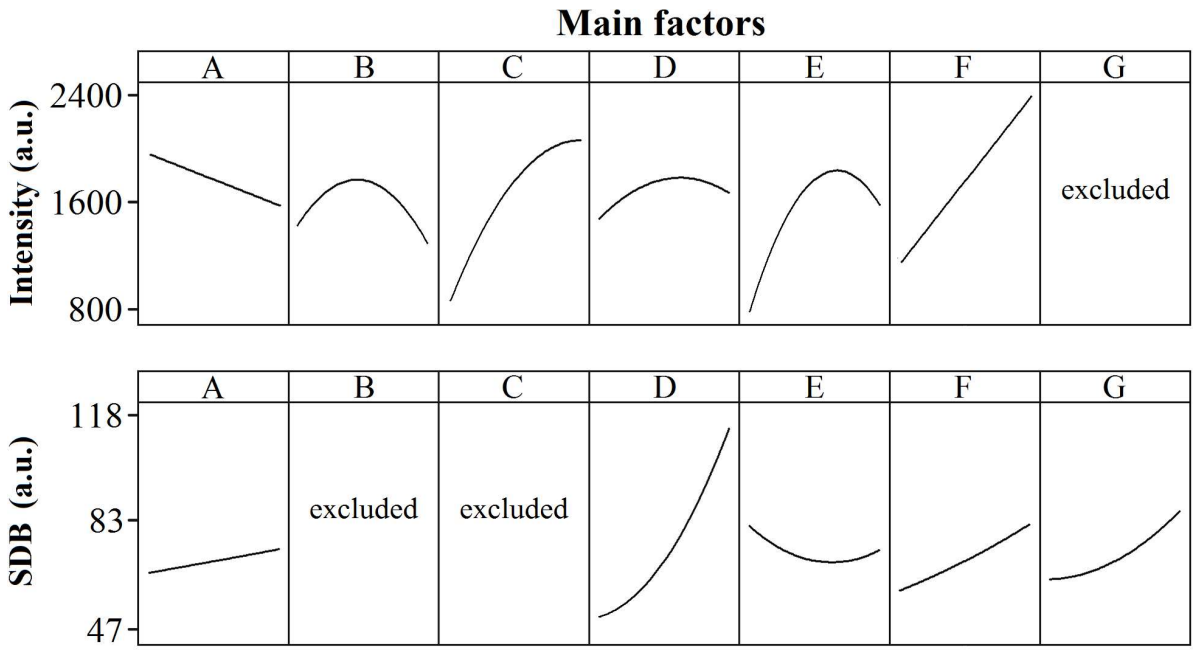

Fig. 5

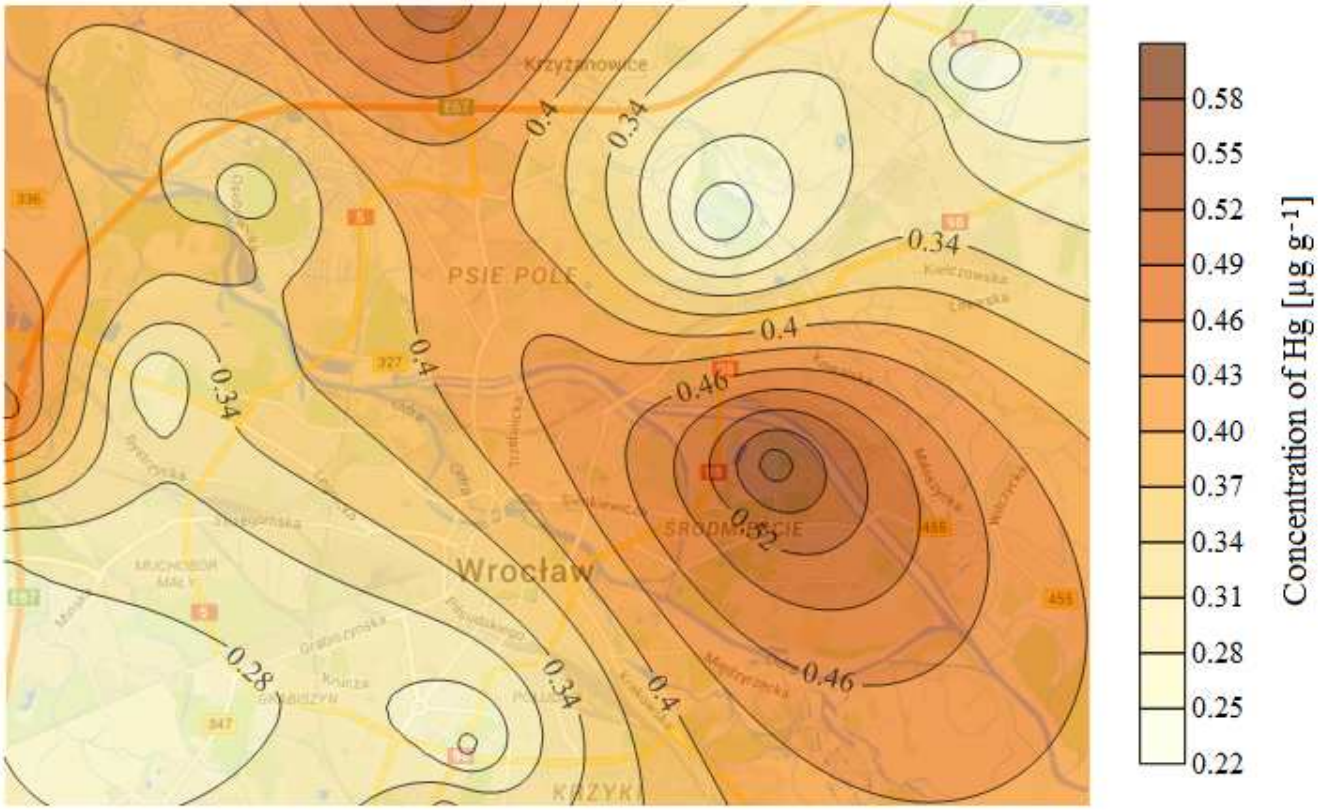

Fig. 6

Graphical abstract